Discrete Element Simulations and Experiments on the Deformation of Cohesive Powders in a Bi-axial Box

O.I. Imole, N.Kumar, V. Magnanimo and S. Luding

Multi- Scale Mechanics, CTW, University of Twente, P. O. Box 217, 7500 AE Enschede, The Netherlands.

Abstract

We present findings from comparison between element test experiments and simulations on the deformation of frictional, cohesive particles in a bi-axial box. We show that computer simulations with the Discrete Element Method can qualitatively reproduce a uniaxial compression element test in the true bi-axial tester. We also highlight the effects of friction and polydispersity on our simulations and present the second stress response namely the deviatoric stress as a function of the deviatoric strain.

1.0 Introduction

Cohesive granular materials are important as raw materials for various commercial applications in the agricultural, geotechnical, pharmaceutical, chemical and food processing industries among others. A great deal of challenge is encountered during the industrial transport, storage, processing and handling of this class of materials due to the contact properties of their constituents. In order to obtain information about the material behaviour, laboratory element test are performed with a control of the stress or strain path. However, they are limited in that they provide little information on the microscopic origin of the behaviour of these complex packings. To overcome this, the Discrete Element Method (DEM) is employed [3]. When all forces acting on a particle, either from other particles, from boundaries or from external forces, are known, the problem is reduced to the integration of Newtons equations of motion for the translational and rotational degrees of freedom.

In this work, we present initial findings from our work focusing on matching Discrete Element simulation of element tests with laboratory experiments on cohesive powders. The element test being considered is the uniaxial deformation mode.

This paper is organized as follows: Section 2 gives a experimental set-up and methodology. In Section 3, we introduce the DEM and the contact model used along with the definition of stress in Section 4. The results are discussed in section 5. Finally, the conclusions are drawn in Section 6.

2.0 Experimental Set-Up and Methodology

The experimental element test being modeled is the true bi-axial box (see Fig. 1) with maximum dimensional size of 130mm x130mm x 65mm which allows the deformation of a brick-shaped bulk solid sample by stress or strain control [9] One advantage of this set-up is the possibility of realising various deformation modes with a single test experiment. The box

comprises of four side plates which can be moved independently while staying perpendicular to the adjacent ones during the deformation of the sample in the x, y or both directions simultaneously. The top and bottom plates are fixed while the complete stress-state on the specimen's border is measured by three load cells installed in the bottom and in the two perpendicular load plates. To ensure that the normal stresses measured at the boundaries are principal stresses (at zero shear stress), flexible rubber membranes are mounted on the four boundaries of the load plates and on the top and bottom plates. Also, silicon grease is applied between the plates and the membranes to minimize friction. This leads to friction coefficients less than 0.02 [10].

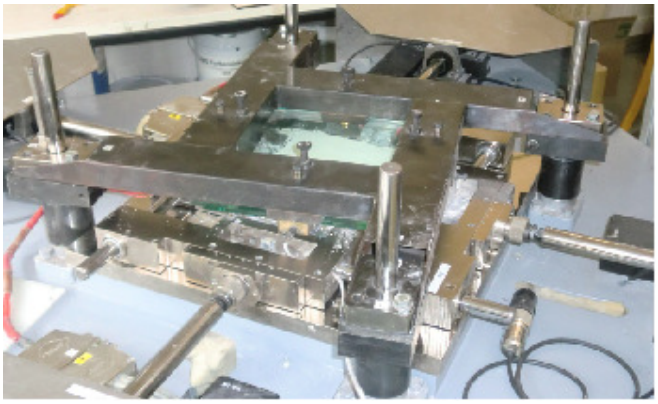

Fig 1: The biaxial box set-up

The sample undergoes a homogenizing 'preparation' stage by an initial bi-axial pre-compaction with the four plates moving inwards in the same direction. This is followed by a quasi-static uni-axial deformation to pre-determined pressure levels.

The cohesive sample used in this work is ESKAL 500 Limestone (KSL Staubtechnik, Germany) with a size range of 10-12 microns and a particle density of 2710kg/m^3. The sample was selected due to its stability under ambient storage condition and minimal degradation under repetitive usage.

3.0 Simulation procedure

The Discrete Element Method (DEM) [2] was used to perform simulations in a bi-axial box. The contact model used is as follows:

$$f_{hys}^{n} = \begin{cases} k_1\delta, & for\ loading, \quad and \\ k_2(\delta - \delta_0) & for\ unloading \end{cases}$$

where for simplicity the loading and unloading stiffness k_1 and k_2 respectively, has been set equal to each other (k_1=k_2) similar to the linear viscoelastic contact model [1]. δ is the overlap between particles. In order to reduce dynamical effects and shorten relaxation times, an artificial background viscous dissipation force is added in the normal and tangential direction, resembling the damping due to a background medium.

3.1 Simulation parameters

Simulation parameters are the system size N =9261= 21^3 particles, density ρ= 2000 [kg/m^3], elastic stiffness k = 10^5 [kg/s^2] and particle damping coefficient = 1 [kg/s]. The static and dynamic friction are set at the same value for all simulations. Ref. [4] provides a description of these artificial units and how they could be rescaled to fit values obtained from experiments. It should also be noted that the system has average particles radius <*r*> = 1 [mm], with polydispersity equal to 3 is quantified by the width of a uniform distribution.

3.2 Initial Configuration

To model the experimental set-up, we generate random particles in a box with periodic boundaries at an initial volume fraction $\nu_0 = 0.3$ and compress the system isotropically to a volume fraction ν_1 above the jamming volume fraction [2], ν_c (the transition from fluid-like behaviour to solid-like behaviour) and subsequently, we allow the system to relax to allow for energy dissipation. A second isotropic compression is initiated from point ν_1 to a target maximum of $\boldsymbol{\nu}_{max}$ and back to the original position. Finally, initial configurations are selected from the unloading branch of this isotropic data to perform the strain controlled uni-axial compression with. Note that quasi-static strain-controlled uni-axial deformation with diagonal strain matrix elements ε_{ii}(0,0,1) is applied in which one wall is moved while the other walls are fixed.

4.0 Stress

The total isotropic stress (pressure) is given as:

$$p = \frac{\sigma_{xx} + \sigma_{\mathrm{yy}} + \sigma_{\mathrm{zz}}}{3} = \frac{1}{3} tr(\sigma)$$

where σ_{xx}, σ_{yy} and σ_{zz} are the diagonal elements of the stress tensor and tr(p) is its trace. The non-dimensional pressure is defined as:

$$p = \frac{2 < r >}{3k} tr(\sigma)$$

where <r> is the mean radius of the spheres and k is the contact stiffness. From the simulations, one can determine the stress tensor as:

$$\sigma^{\alpha\beta} = \frac{1}{V}\left(\sum_{p \epsilon V} m_p v_p^{\alpha} v_p^{\beta} - \sum_{c \epsilon V} f_c^{\alpha} l_c^{\beta}\right)$$

with particle p, velocity vp, contact c, force fc and branch vector lc while Greek letters represent components. The sum includes the kinetic energy of the particles and the contact force dyadic product with the branch vector, in the vicinity of the averaging volume, weighted according to their vicinity. In this study, since we focus on averages over the total volume, the weighting is irrelevant and the sum runs over all the particles and contact.

5.0 Results

5.1 Experiment

Fig. 2(a) shows the evolution of pressure as a function of time during the uniaxial compression of limestone powder. The experiment was conducted in four phases as follows. First, a biaxial compression in the x and y direction resulting in a steady increase in the pressure until 10kPa is reached. An increase in pressure is also observed in the non-moving z direction though the rate of increase is not as rapid as in the other two active directions. This is followed by a relaxation phase for 300sec characterized by a creep-like 30 percent drop in pressure with the wall position still in place. This time-dependent behavior is a feature of cohesive solids [9] and will be studied in details elsewhere.

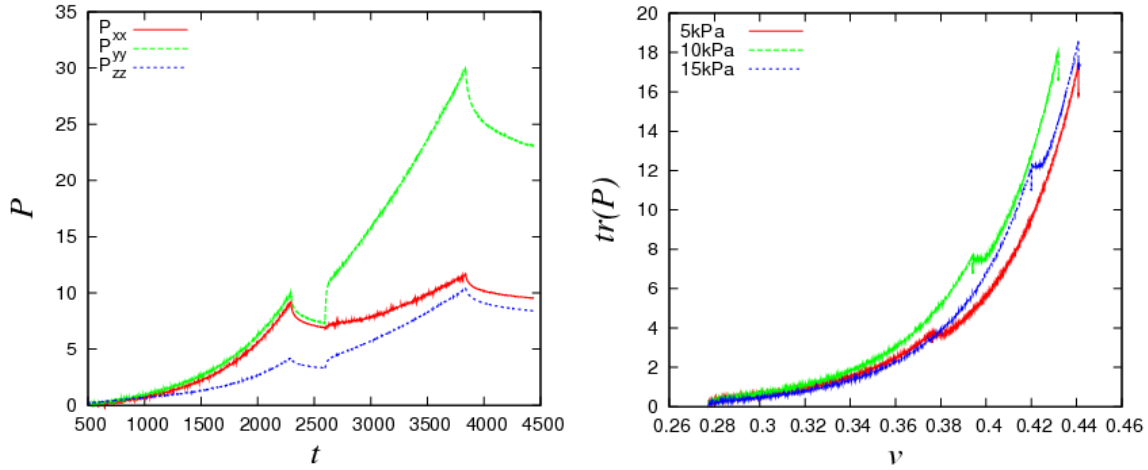

Fig. 2(a): Plot of pressure as a function of time during biaxial compression, relaxation and uniaxial compression followed by another relaxation. Legend represents the pressure on the x, y and z directions. Fig. 2(b): Plot of the total average pressure against volume fraction for three biaxial preparation pressures shown in the legend during uniaxial compression. Only the active uniaxial compression direction is shown.

Uniaxial compression is initiated after the relaxation until a target pressure of 30kPa is reached. At this stage, compression is only in the y-direction while the x and z directions remain immobile though a slight increase in pressure is also seen. Finally, another relaxation is performed at the end of the uniaxial compression cycle for 1000secs leading to a drop in pressure by about 26 percent.

The average pressure (trace) plotted as a function of volume fraction is shown in Fig 2(b) for three biaxial preconsolidation pressures. In this case, only the most active deformation direction is shown. The most active direction is the direction from which the uniaxial compression is performed. The volume fraction is defined as the dimensionless ratio of the bulk density and the particle density. As seen, pressure increases with increasing volume fraction until the target pressure is reached. The short vertical bumps seen on each plot show the intermediate and final relaxation cycle since pressure drops at constant volume fraction.

5.2 Simulation

The effects of friction and polydispersity on the jamming transition are highlighted in the plot of pressure as a function of volume fraction in Figs. 3(a-b). The polydispersity index *w* is defined as the ratio between the largest and smallest particle radii ($w=r_{max}/r_{min}$). As seen from Figs. 3(a-b), an increase in the polydispersity generally leads to an increase in the isotropic jamming density [2]. On the other hand, increasing friction slightly from μ=0 to μ=0.1 leads to a decrease in the jamming volume fraction since friction encourages a more compact packing.

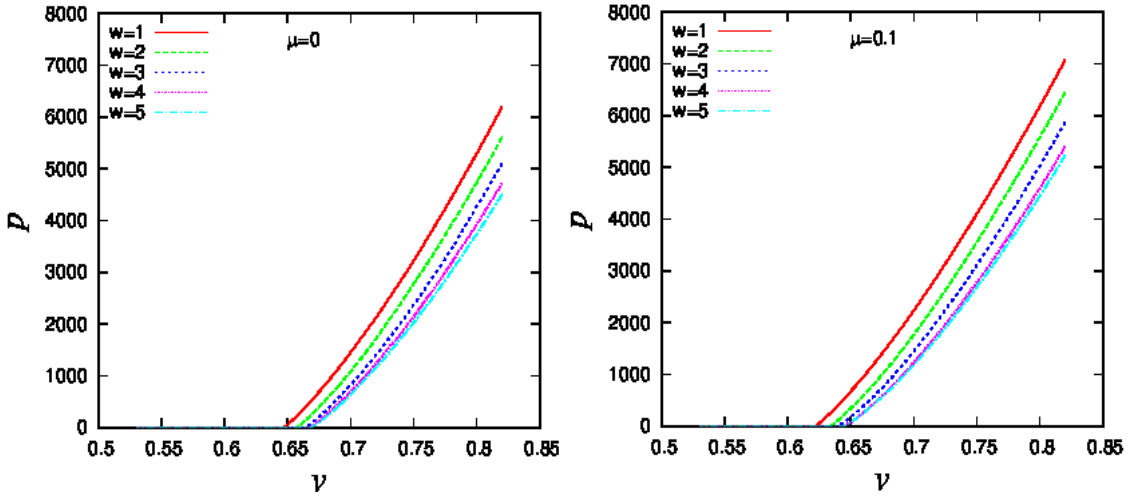

Fig. 3(a): Plot of pressure as a function of volume fraction with μ=0 and polydispersity *w=1,2… 5. 3(b) same dataset* for μ=0.1.

5.3 Deviatoric Stress

The most objective form to calculate the shear stresses [7] for any 3D geometry that accounts for triaxial deformation is defined as:

$$\sigma_{dev} = \sqrt{\frac{(\sigma_{xx}-\sigma_{yy})^2 + (\sigma_{yy}-\sigma_{zz})^2 + (\sigma_{zz}-\sigma_{xx})^2}{2}}$$

where σ_{xx}, σ_{yy} and σ_{zz} are as defined earlier. The deviatoric strain can also be defined as:

$$\varepsilon_{dev} = \sqrt{\frac{(\varepsilon_{xx}-\varepsilon_{yy})^2 + (\varepsilon_{yy}-\varepsilon_{zz})^2 + (\varepsilon_{zz}-\varepsilon_{xx})^2}{2}}$$

where ε_{xx}; ε_{yy} and ε_{zz} are the diagonal elements of the strain matrix. The factor 2 used in the denominator is a matter of choice as it only leads to a change in the value of the maximum deviatoric stress obtained at saturation. The deviatoric response of a frictional simulation is

shown in Fig. 4 with the compression beginning from five different initial volume fractions as shown in the legend. The deviatoric stress has been normalized with the average isotropic stress (pressure); defined as $S_{dev} = \sigma_{dev}/p$. Interestingly, the evolution of the stress-ratios is very similar for the different deformation modes.

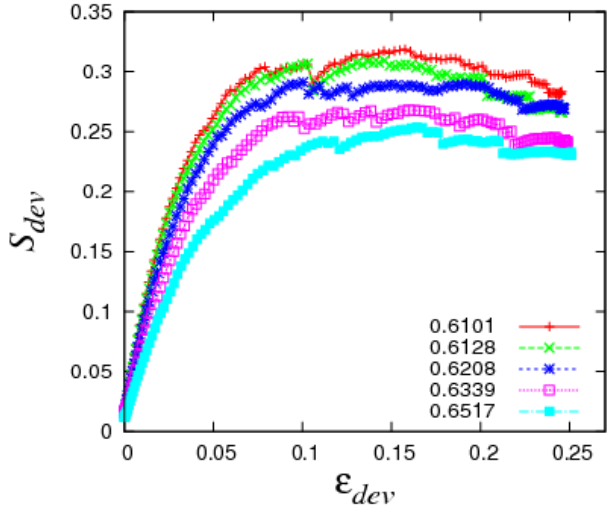

Fig. 3(a): Evolution of the deviatoric stress as a function of the deviatoric strain during uniaxial loading. The Inset shows the different volume fractions from which the simulations were initiated.

Also, the slope of the normalized deviatoric stress function against deviatoric strain reduces as the volume fraction is increased, unlike the classical shear modulus G [5], which increases with volume fraction [6, 7], as consistent with findings from macroscopic experiments with shear testers [8].

Conclusion

We have presented experimental and numerical results from the uniaxial deformation o frictional particles in a bi-axial box. From the simulations performed, we have shown that an increase in friction generally leads to a decrease in the isotropic jamming point while increasing polydispersity leads to a corresponding increase in the jamming density. Aside the fact that the jamming transition must be exceeded before meaningful pressure evolution can be seen, the profiles of the evolution of pressure as a function of volume fraction for the laboratory element test experiments with the biaxial box qualitatively agrees with the DEM simulations. In future, quantitative agreements between experiments and simulations will be explored with the implementation of the truly hysteretic contact model and the inclusion of cohesion.

Acknowledgement

The support of the European Community under the Marie Curie Initial Training Network is gratefully acknowledged

References

[1] Luding, S., and Perdahcioglu, S., “A local constitutive model with anisotropy for various homogeneous 2D Biaxial deformation modes”, CIT 83(5), pp. 672-688, 2011.
[2] Göncü, F., Duran, O., and Luding, S., “Constitutive relations for the isotropic deformation of frictionless packings of polydisperse spheres”, C. R. Mecanique, 338, pp. 570-586, 2010.
[3] Cundall P.A., Strack, O.D.L., “A discrete numerical model for granular assemblies”. Geotechnique, 29, pp. 47-65, 1979.
[4] Luding, S., “Cohesive, frictional powders: contact models for tension,” Granular Matter, 10, pp. 235-246, 2008.
[5] Magnanimo, V. and Luding, S., “A local constitutive model with anisotropy for ratcheting under 2D biaxial isobaric deformation “, Granular Matter, 13, No. 3, pp. 225-232.
[6] Imole, O. I., Kumar, N. and Luding, S., “Deformation modes of packings of frictionless polydisperse spheres” in press, PSA2011 proceedings, Edinburgh, 5-7 Sept., 2011
[7] Imole, O. I., Kumar, N. and Luding, S., “Different deformation modes of 3 dimensional packings of frictionless polydisperse spheres” in preparation.
[8] Schwedes, J. and Schulze, D., ‘‘Measurement of flow properties of bulk solids”, Powder Technology, 61, pp. 59–68, 1990
[9] Zetzener H., and Schwedes, J. Deformation behaviour and relaxation of bulk solids at different deformation rates. 6th Intl. Conf. on Handling and Transportation, pages 51{55, 1998.